An Analytical Method for Designing Embedded Retaining Walls

Lysandros Pantelidis(✉)

Cyprus University of Technology, Limassol, Cyprus
lysandros.pantelidis@cut.ac.cy

Abstract. Intermediate earth pressures act on the wall when the latter has not moved enough so that the active or passive state to be reached. These pressures are of particular importance for designing embedded retaining walls; embedded walls are flexible structures and along their length different soil state may exist at the same time. Very recently, the author proposed a continuum mechanics approach for deriving earth pressure coefficients for any soil state between the at-rest state and the active or passive state, applicable to cohesive-frictional soils and both horizontal and vertical pseudo-static conditions. The same method also provides analytical expression for the calculation of the required wall movement (at any depth) for the mobilization of the active or passive failure state. In the present paper the author suggests a new, fully analytical method for designing embedded retaining walls, combining the proposed method with the elastic beam theory. An application example is given along with comparison with the finite element method.

Keywords: intermediate earth pressures · the Generalized Coefficient of Earth Pressure · elastic beam theory

1 Introduction

Intermediate earth pressures act on the wall when the latter has not moved enough so that the active or passive state to be reached. These pressures are of particular importance for designing embedded retaining walls; embedded walls are flexible structures and along their length different soil state may exist at the same time. The methods included in a standard are supposed to reflect the best (current) practice. In 2001, BS 8002 [1] outlined five "traditional" methods for designing embedded walls, mentioning, however, that all these methods have serious shortcomings and limited applicability. These methods are: a) the gross pressure method, b) the net available passive resistance method, c) the strength factor method, d) the nett pressure method and e) the end fixity method. The more recent EN1997-1:2004 [2] and prEN1997-3:2022 [3] (draft standard), on the other hand, suggest that intermediate values of earth pressures be calculated using empirical rules (e.g., interpolation), beam on springs models, or continuum numerical models. However, the beam on springs models is also highly empirical, as empirical rules are used for determining the spring constant. Apparently the simplistic and empirical nature of

R. E. Hammah et al. (Eds.): RIC 2023, AHE 19, pp. 217–224, 2023.
https://doi.org/10.2991/978-94-6463-258-3_23

the above approaches raise serious queries about their validity. Thus, it seems that among the above, the best alternative is numerical modelling. However, the intermediate earth pressures highly depend on the initial stresses set in the program; the latter are not always correctly defined, especially for soils having cohesion or being overconsolidated. On the other side of the ocean (e.g., [4, 5]), things seem to be pretty much the same. The purpose of the present paper is to suggest a reliable method for designing embedded retaining walls. The new method is based on the Generalized Coefficient of Earth Pressure recently proposed by the author [6], combining the theory of elastic beams from statics.

2 The Generalized Coefficient of Earth Pressure

In 2019, the author [6] derived an earth pressure coefficient for any soil state between the at-rest state and the active or the passive state, applicable to cohesive-frictional soils and both horizontal and vertical pseudo-static conditions, through a continuum mechanics procedure. The basic earth pressure coefficient expression is:

$$K_{XE} = \frac{1-(2\lambda-1)\sin\varphi_m}{1+(2\lambda-1)sin\varphi_m} - (2\lambda-1)\frac{2c_m}{(1-a_v)(\sigma_v-u)}\tan\left(45^o-(2\lambda-1)\frac{\varphi_m}{2}\right) \tag{1}$$

where, c_m and φ_m are the mobilized shear strength parameters of soil, a_v is the vertical pseudo-static coefficient, u is the pore water pressure and σ_v is the vertical total stress. λ is a soil state coefficient being either 0 or 1, while $X = O, A, P, IA$ or IP denoting the at-rest, active, passive, intermediate active and intermediate passive state respectively. The readers should bear in their mind that the "Rankine's" form of Eq. 1, came naturally through the continuum mechanics procedure followed. The mobilized cohesion of soil, c_m, and the mobilized internal friction angle of soil, φ_m, are calculated using Eqs. 2 and 3 respectively.

$$c_m = c'\frac{\tan\varphi_m}{\tan\varphi'} \tag{2}$$

$$\varphi_m = Re\left(\sin^{-1}\left(-(2\lambda-1)\frac{b_o+\frac{D_0}{C_0\zeta^\lambda}+C_0\zeta^\lambda}{3\alpha_o}\right)\right)\frac{180}{\pi}(^\circ) \tag{3}$$

where, $a_o = \left(1+e_2^2\tan^2\varphi'\right)$, $b_o = 1-(2(2\lambda-1)e_1e_2+e_2^2)\tan^2\varphi'$, $c_o = (e_1^2+2(2\lambda-1)e_1e_2)\tan^2\varphi'$, $d_o = -e_1^2\tan^2\varphi'$, $D_0 = b_o^2-3a_oc_o$, $D_1 = 2b_o^3 - 9a_ob_oc_o+27a_o^2d_o$, $C_0 = \sqrt[3]{\frac{1}{2}\left(D_1-\sqrt{D_1^2-4D_0^3}\right)}$, $e_1 = (1-A_0)/B_1$, $e_2 = (1+A_0)/[(2\lambda-1)B_1]+2c'/\left[(1-a_V)(\sigma_v-u)(2\lambda-1)B_1\tan\varphi'\right]$, and $\zeta = -1/2+\left(\sqrt{3}/2\right)i$. The Re notation in Eq. 3 means that only the real part of the number is kept; the imaginary part (if any) is infinitesimally small, and thus, zero.

For the active "side" of the problem (state at-rest to the active state), $\lambda = 1$ and

$$A_0 = \frac{1-\sin\varphi\prime}{1+\sin\varphi\prime}\left(1-\xi\sin\varphi\prime+\tan\theta_{eq}\tan\varphi\prime(2+\xi(1-\sin\varphi\prime))\right) \tag{4}$$

$$B_1 = \frac{2c\prime}{(1 - a_v)(\sigma_v - u)} \tan\left(\frac{\pi}{4} - \frac{\varphi\prime}{2}\right) \quad (5)$$

For the passive "side" of the problem (state at-rest to the passive state):

$$A_0 = \left(\frac{1 + \sin\varphi\prime}{1 - \sin\varphi\prime}\right)^{\xi_1} \left(1 + \xi \sin\varphi\prime + \xi_2 \tan\theta_{eq} \tan\varphi\prime (2 + \xi(1 + \sin\varphi\prime))\right) \quad (6)$$

$$B_1 = (2\lambda - 1) \frac{2c\prime}{(1 - a_v)(\sigma_v - u)} \tan^{\xi_3}\left(\frac{\pi}{4} + \frac{\varphi\prime}{2}\right) \quad (7)$$

where, $\lambda = 0$ or 1 when $A_0 \geq 1$ or ≤ 1 respectively, $\xi_1 = 1 + \xi$, $\xi_2 = 2/m - 1$ and $\xi_3 = 1 + 2\xi$. ξ_1, ξ_2 and ξ_3 are parameters related to the transition from the soil wedge of the state at-rest to the soil wedge of the passive state.

Generally, $\theta_{eq} = a_H/(1 - a_V)$ (a_H is the horizontal pseudo-static coefficient), while for both active and passive "sides", $\xi = -2/(m + 1)$. m is a real positive number (ranging from 1 to $+\infty$) calculated as follows:

$$m = \left(1 + \left(\Delta y / \Delta y_M\right)(H/z)^{1+\Delta y/\Delta y_M}\right)\left(1 - \Delta y / \Delta y_M\right)^{-1} \quad (8)$$

m, in essence, defines any intermediate state on the active or the passive "side" of the problem. Δy_M is the required horizontal displacement for the development of the active or passive state at the mid-height of the retained soil, that is, $\Delta y_M = \Delta y_{max}(z/H = 0.5)$. F or0 $\leq z/H \leq 0.5$, Δy_{max} is calculated using Eq. 9. For $0.5 \leq z/H \leq 1$, Δy_{max} has constant value, which is equal to the one corresponding to $z/H = 0.5$.

$$\Delta y_{max} = \frac{\pi}{4} \frac{\left(1 - \nu^2\right)}{\mathrm{E}} \frac{(1 + z/H)^3 (1 - z/H)}{z/H} H \cdot \Delta K \cdot (1 - a_v)(\sigma_v - u) \quad (9)$$

$\Delta K = K_{OE} - K_{AE}$ or $K_{PE} - K_{OE}$, depending on the case examined while E and ν are the elastic modulus and Poisson's ratio of the retained soil. Δy_{max} becomes maximum for $z/H = 0.5$. Δx in Eq. 8 is the deflection of the wall at any depth z, calculated based on the elastic beam theory.

The total earth pressure (at any depth) acting perpendicular to a vertical or nearly vertical retaining structure for any soil state X, therefore, is

$$\sigma_{XE} = K_{XE}(\sigma_v - u) + u \quad (10)$$

An exhaustive validation of Pantelidis' [6] continuum mechanics method against contemporary centrifuge tests and finite elements can be found in Pantelidis and Christodoulou [7]. The above formulae will be used herein for introducing a new method for designing embedded retaining walls.

3 Application Example and Numerical Validation

The analysis that follows combines the earth pressure method proposed by the author [6] and the elastic beam theory (simple cantilever beam). The example presented herein has been solved both with the proposed analytical method (using KWall v.1 educational software prepared by Dr Panagiotis Christodoulou and the author) and with Rocscience's RS2 (for validation purposes). The geometry, mesh and boundary conditions of the problem are shown in Fig. 1. The wall is free to bend from $z = 0$ to 10 m, while below the $z = 10$ m depth point, the wall is practically fixed. In the analytical procedure both the translational and rotational components of movement was assumed zero. In the numerical procedure, the anchorage of the wall was achieved setting a horizontal nodal displacement as low as 0.1 mm for $z = 10$ *to* 15 m. This very small nodal displacement was imposed in the lower five meters of the wall instead of using a very stiff soil layer for obtaining more stable results. The wall which has flexural rigidity $E_W I_W = 1.5\text{GPa} \cdot \text{m}^4$ functions in a homogenous, isotropic mass with cohesion $c' = 0$ kPa, internal friction angle $\varphi' = 30°$, unit weight $\gamma = 20$ kN/m^3, Young's modulus $E = 20$ MPa and Poisson's ratio $\nu = 0.3$. Pore-water pressures and seismic excitation was ignored for the sake of simplicity.

Favoring reproduction of the example problem, all relevant information is given below (if something is not mentioned, the RS2 default value was used). The "*Gaussian elimination*" solver type was used. Regarding the "*stress analysis*" menu, the maximum number of iterations was 1000, the tolerance was set to 0.001, while the "*comprehensive*" convergence type was adopted. The "*mesh type*" was set to "*graded*", while 6-noded triangular elements were used (meaning 19.0 nodes/m^2 or 9.2 elements/m^2; see Fig. 1). The "*field stress type*" was "*gravity*" with "*stress ratio*" in- and out-of-plane equal to 0.5 (recall Eq. 1 for the soil considered, $\Delta x = 0$ m and $a_H = a_V = 0$). The "*initial element loading*" was "*field stress and body force*". The problem was solved statically ($a_H = a_V = 0$). The soil parameters were those given earlier (apparently, the "*plastic*" material type was chosen). The wall was modeled as "*structural interface*", with a "*standard beam*" element as liner and a "*joint*" element on both sides. The liner was considered to be "*elastic*" with Young's modulus $E_w = 15 \cdot 10^6$ kPa and thickness 1.0627 m (moment of inertia $I_w = 1.0627^3 \cdot 1/12 = 0.1$ m^4); this combination of values gives the $E_w I_w =$

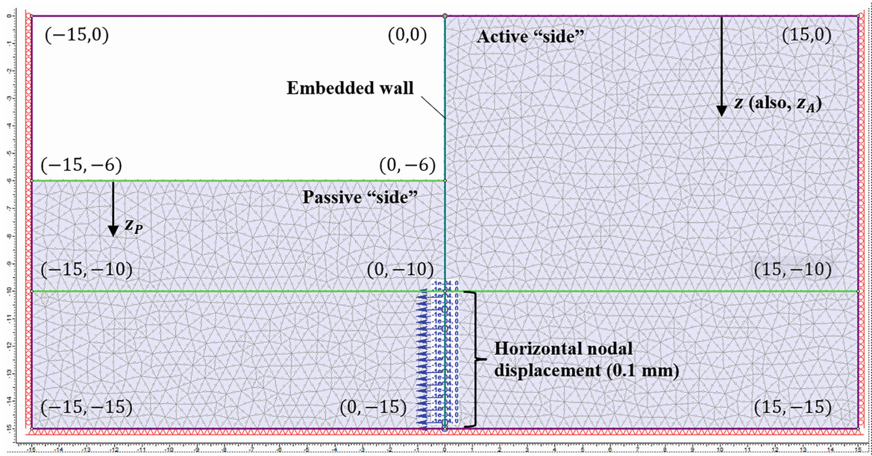

Fig. 1. Geometry of the problem. Also, geometry, mesh and boundary conditions of the RS2 model used

$1.5 \cdot 10^6$ kPa·m^4 (beam stiffness) value used by the author in the analytical solution (the Poisson's ratio of the liner was 0.01, while the "*Timoshenko*" beam element formulation was adopted). Regarding "*joint*", the "*material dependent*" slip criterion was chosen with "*interface coefficient*" as low as 0.05 (it is reminded that the proposed earth pressure analysis method is for smooth walls. Both the normal and shear stiffness of the joint element was set to 200 MPa/m.

Regarding the proposed analytical procedure, the deflection Δy (at any depth z) is calculated based on the elastic beam theory, where the embedded wall of Fig. 1 is treated as a cantilever beam; the earth pressures on the two sides of the wall constitute the loading acting on the beam, where the principle of superposition stands. An iterative procedure is needed. As a starting point (1st iteration), it is logical and convenient to assume that the soil on both sides of the wall is at the state at-rest (that is, $\Delta y = 0$ m, meaning that Eq. 1 is applied for $m = 1$). However, since $H_A > H_P$, this state, cannot be true (at least for the majority of points along the wall); the embedded wall will have the tendency to bend towards the passive "side" (controlled more or less by the flexural rigidity of the wall). The deflection (Δy_{tot}) of the wall caused by the combined action of the earth pressure distributions acting on the two sides of the wall is then calculated. For the 2nd iteration these Δy_{tot} values are the Δx data values and so on, until convergence to be achieved. Five iterations were adequate for obtaining stable results. The final results, as these have been obtained in the last (5th) iteration are shown in chart form in Figs. 2 and 3.

In the chart of Fig. 2 the analytically and numerically derived deflection values of the wall have been drawn against depth; the $\Delta y_{max,A}$ and $\Delta y_{max,P}$ values (for the active and passive state respectively) are also shown on the same chart. In this respect, a number of observations can be made: a) the proposed method effectively calculated the deflection

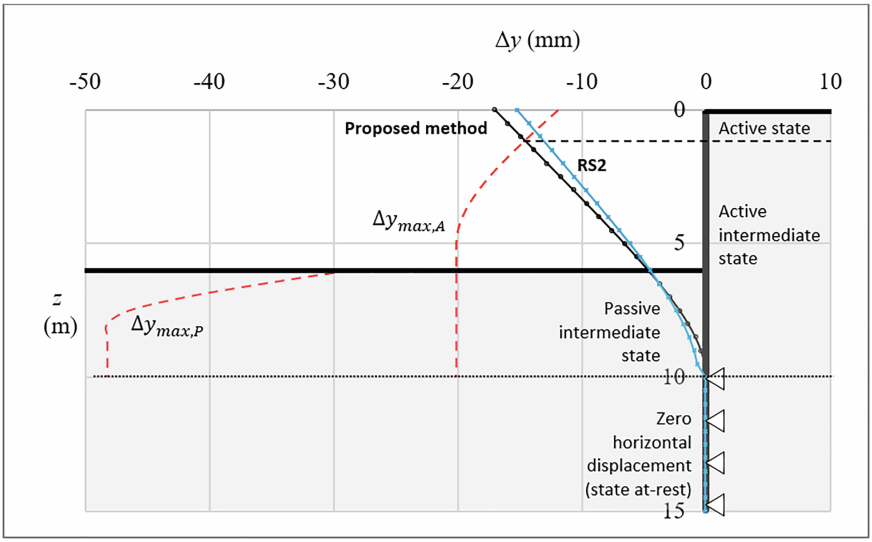

Fig. 2. Deflection of embedded wall versus depth chart

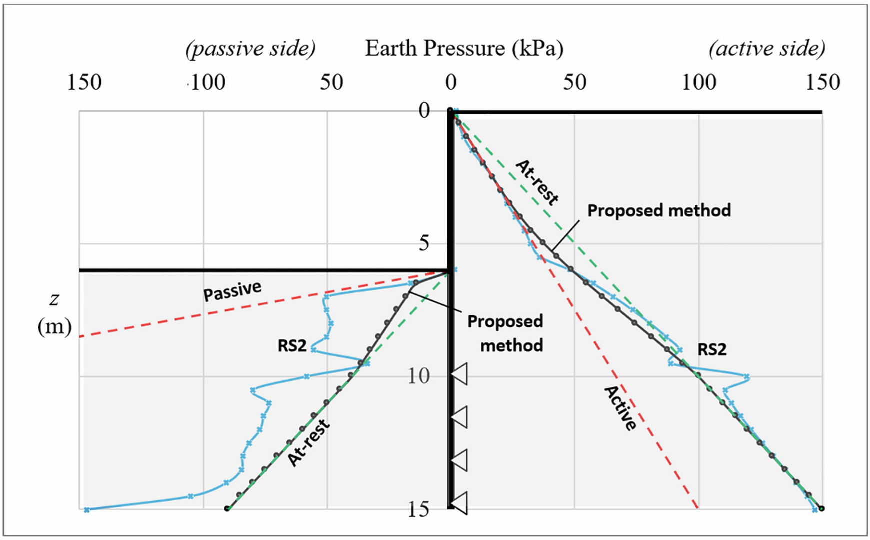

Fig. 3. Chart showing the earth pressures on both sides of the embedded wall. The dashed lines simple indicate the "active", "passive" and "at-rest" state

of the embedded wall, b) an active failure state zone exists near the top of the wall ($\Delta y_{tot} \geq \Delta y_{max,A}$), while for the rest of the soil mass adjacent to the wall, the soil is at an intermediate active or passive state, and d) the analytical solution shows that the soil on the passive "side" of the problem is far from failure; besides, a deflection as low as 4.5 mm (maximum deflection, referring to $z_P = 0$ m) is not able to cause an active failure in the spesific soil, let alone a passive one.

The analytical and numerical earth pressure distributions have been drawn against depth in Fig. 3. As shown, the two "active" curves (the analytical and the numerical ones) match very well to each other. Also, as expected, for $z > 10$ m (that is, for z below the theoretical fixed point of the wall), both curves coincide with the theoretical earth pressure at-rest distribution. For the passive state the analytical curve shows earth pressures closer to the respective earth pressures at-rest, something that can be justified by the small deflection values with respect to the respective $\Delta y_{max,P}$ threshold values. The "passive" numerical curve, on the other hand, shows a very peculiar behavior with great intermediate earth pressure values which, indeed, for $6m < z < 7m$ ($0m \leq z_P \leq 1m$) are extremely close to the passive state ones. In addition, for $z > 10$ m, where the wall has been held practically still, the numerical earth pressures are (much) greater than the logically expected earth pressures at-rest. Apparently, the earth pressure at-rest values on the active "side" should also stand for the passive "side"; this discrepancy has to do with the numerical procedure and cannot be explained by the author.

4 Conclusions

The knowledge of intermediate earth pressures (i.e., earth pressures between the at-rest state of soil and the active or the passive one) is very important in designing embedded retaining structures. However, in the absence of a reliable method for calculating these pressures (which depend on the amount of movement and bending of the flexible wall), the various design standards worldwide rely on simplistic approaches, major assumptions and empirical rules and parameters. This way of dealing with intermediate earth pressures was so far a "necessary evil", with the reliability of the results to rather be under dispute.

In this paper a new, fully analytical method for designing embedded retaining walls has been suggested. This combines the earth pressure theory proposed in 2019 by the author with the elastic beam theory. An application example is given, indicating remarkable agreement with the finite element method. The effectiveness of the proposed method refers not only to the calculation of the earth pressures but also to the calculation of the deflection profile of the wall. Comparison with the finite element method showed excellent agreement. Indeed, a great advantage of the proposed method against finite elements is the stability of the results.

Finally, given the rationality and the effectiveness of the proposed method, the latter could replace the existing crude and semi-empirical methods which not only lacks solid theoretical basis but also, thorough calibration and thus, leading to more cost effective and more reliable structures.

References

1. BS 8002:1994, Code of practice for earth retaining structures, British Standard (2001).
2. EN 1997-1, Eurocode 7: Geotechnical design - Part 1 General rules, European Standard (2009).
3. prEN1997-3:2022, Eurocode 7: Geotechnical design - Part 3: Geotechnical structures, European Standard (2022).
4. FHWA-NHI-07-071, Earth Retaining Structures - Reference Manual, U.S. Department of Transportation Federal Highway Administration (2008).
5. Canadian Geotechnical Society, Canadian Foundation Engineering Manual 4th ed. (2006).
6. Pantelidis, L.: The Generalized Coefficients of Earth Pressure: A Unified Approach. Appl. Sci. 9, 5291 (2019).
7. Pantelidis, L., Christodoulou, P.: Comparing Eurocode 8–5 and AASHTO methods for earth pressure analysis against centrifuge tests, finite elements, and the Generalized Coefficients of Earth Pressure. ResearchSquare (preprint), (2022). https://doi.org/10.21203/rs.3.rs-1808466/v3